Climatic Change (2007) 83:151–168
DOI 10.1007/s10584-006-9232-1

Frequency and duration of historical droughts from the 16th to the 19th centuries in the Mexican Maya lands, Yucatan Peninsula

Blanca Mendoza · Virginia García-Acosta · Victor Velasco · Ernesto Jáuregui · Rosa Díaz-Sandoval

Received: 23 June 2006 / Accepted: 28 November 2006 / Published online: 8 March 2007

Abstract Using unprecedented catalogues of past severe drought data for the Yucatan Peninsula between 1502 and 1900 coming from historical written documentation, we identified five conspicuous time lapses with no droughts between 1577–1647, 1662–1724, 1728–1764, 1774–1799 and 1855–1880, as well as time epochs with most frequent droughts between 1800 and 1850. Moreover, the most prominent periodicity of the historical drought time series was that of ~40 years. Using the Palmer Drought Severity Index for the Yucatan Peninsula for the period 1921–1987 we found prominent negative phases between ~1942–1946 and 1949–1952, 1923–1924, 1928–1929, 1935–1936, 1962–1963, 1971–1972 and 1986–1987. Two prominent periodicities clearly appear at ~5 and 10 years. Most modern and historical severe droughts lasted 1 year, and share a quasi-decadal frequency. Also, in the first 66 years of the twentieth century the frequency of occurrence of severe drought has been lower compared with the nineteenth century. Some of the major effects and impacts of the most severe droughts in the Yucatan region are examined. We also studied the relation between historical and modern droughts and several large scale climate phenomena represented by the Atlantic Multidecadal Oscillation (AMO) and the Southern Oscillation Index (SOI). Our results indicate that historical droughts and the cold phase of the AMO coincide, while the influence of the SOI is less clear. The strongest coherence between historical droughts and AMO occurred at periodicities of ~40 years. For modern droughts the coherence of a drought indicator (the Palmer Drought Severity Index) is similar with AMO and SOI, although it seems more sustained with the AMO. They are strongest at ~10 years and very clearly with the AMO cold phase. Concerning the solar activity proxies and historical droughts, the coherence with a record of

B. Mendoza (✉) · V. Velasco · E. Jáuregui · R. Díaz-Sandoval
Instituto de Geofísica, Universidad Nacional Autónoma de México,
Ciudad Universitaria, 04510 México, D.F., México
e-mail: blanca@geofisica.unam.mx

V. García-Acosta
Centro de Investigaciones y Estudios Superiores en Antropología Social, Juárez 87,
14000 México, D.F., México
e-mail: dirgral@ciesas.edu.mx

beryllium isotope Be^{10}, which is a good proxy of cosmic rays, is higher than with Total Solar Irradiance. We notice that the strongest coherence between historical droughts and Be^{10} occurs at periods ~60–64 years. When studying modern droughts and solar activity, frequencies of ~8 years appear, and the coherences are similar for both sunspots and cosmic rays. Comparing natural terrestrial and solar phenomena, we found that the most sustained and strongest modulation of historical drought occurrence is at ~60–64 years and is between the historical drought series and the solar proxy Be^{10}. For modern droughts we notice that the coherence is similar among AMO, SOI and the solar indices. We can conclude that the sea surface temperatures (AMO) and solar activity leave their signal in terms of severe droughts in the Maya lands, however in the long term, the influence of the SOI on this type of phenomenon is less clear.

1 Introduction

Historical climate studies on time scales of centuries to millennia provide a very valuable basis for interpreting the present climate behavior and to assess future effects of climate change.

Instrumental records of temperature in most places have been available since approximately the last century. In addition, proxy climate indices such as tree ring chronologies, ice cores, lake sediments, etc. have been used in order to reconstruct past climates. Other types of proxy climate information used are diaries, archives, chronicles, old newspapers, as well as iconographical and bibliographical material.

In Mexico, instrumental temperature records are available from the late nineteenth century (see review by Jáuregui 1997). Recently a catalogue of Agricultural Disasters for Mexico has been prepared containing an unprecedented amount of historical data along almost six centuries of Mexican history (García-Acosta et al. 2003; Escobar 2004); it includes droughts among other records related to the so-called agricultural disasters, coming mainly from primary written sources.

Taking advantage of this catalogue, in the present paper we explore the behavior of historical droughts in the Yucatan Peninsula and attempt to study their possible association to natural phenomena such as the Atlantic Multidecadal Oscillation (AMO), the Southern Oscillation Index (SOI) and some solar activity associated phenomena.

2 Present climate

The climate of Mexico is influenced by the position and strength of the subtropical high pressure systems of the North Atlantic and the North East Pacific oceans (centred near 30° latitude), as well as by the location of the inter-tropical convergence zone lying to the south of the country. While moist trade winds prevail during the half year centred in summer, penetration of polar continental air masses from North America occurs in winter and spring resulting in a marked drop of temperature in most of the country (Klaus 1973; Jáuregui 1995). The intrusion of cold air in the Yucatan peninsula is associated with strong northerly winds called “Nortes” producing occasionally intense precipitation. The rainfall regime in the southern parts of the country has usually two maxima, one in June and the other in September. Meanwhile July and August show a decline in convective activity known as canícula or midsummer drought (e.g., Mosiño and Garcia 1966; Magaña et al. 1999). This bimodal variation of rainfall appears to be the result of changes in the intensity of the low-

level winds during July and August blowing over a region of warm waters off the Pacific coast of southern Mexico, known as the "warm pool" where convective activity is intense (Magaña et al. 2003). Cloud cover variations are likely to modulate the sea surface temperature of these seasonally warm waters. Magaña et al. (1999) note that after the onset of the summer monsoon around May–June the sea surface temperature over the eastern Pacific decreases by around 1°C due to interception of solar radiation by the increasing cloudiness and enhanced evaporation by stronger easterly winds. Such sea surface temperature changes result in a substantial decrease in deep convective activity during July and August in the region.

Variability of temperature and precipitation in the Yucatan region during the winter months is strongly modulated by outbreaks of polar air masses, which sweep southward with strong northerly winds, and are known as "Nortes." Such intrusions of air masses of polar origin with high winds across the Yucatan peninsula, as well as over the mountains of Chiapas and eastern Oaxaca states and through the Istmus of Tehuantepec are a characteristic feature of the winter climate in our study region. The weather events that are associated with the more severe cold frontal passages include gale force winds, torrential rains and extreme temperature fluctuations; they have been discussed by for instance Di Mego et al. (1976), Colle and Moss (1995) and Schultz et al. (1997). In particular, Di Mego et al. have presented maps showing the mean monthly frequency of frontal passages comprising the whole Mexico–Caribbean region, where it is clear that these systems may reach as far as southern parts of Central America.

While most of the precipitation in the Yucatan Peninsula fall during the summer rainy season of May–October, drought in the region can develop from a prolonged period of below average rainfall affecting either or both wet and dry seasons.

3 Historical drought series

In this paper we use a different and more extended historical drought data for the Yucatan Peninsula that the one used in previous works (i.e. Mendoza et al. 2005, 2006). The records for historical droughts come mainly from the following catalogues: García-Acosta et al. (2003) that refer to agricultural disasters in general, including droughts, between 958 and 1822. Escobar (2004) that also refers to agricultural disasters in general, including droughts, from 1822 to 1900. The data has been supplemented with information from Farriss (1992), about epidemics and famine in colonial Yucatan between 1535 and 1820, and Bracamonte (1994) that records droughts between 1742 and 1855. They constitute a unity for the period 1502–1900, and will be referred in this paper as the Catalogue.

The Catalogue is made up of two types of records, according to their origin or to their location. As such, they are primary or secondary data, they come from archives or they are bibliographical, journalistic or iconographical data. The main sources for primary historical data are archives. The Catalogue includes information coming from near 50 Mexican archives (mainly official ones) as well as from two located beyond Mexican frontiers (Archivo General de Indias, Spain and Archivo General de Centroamérica, Guatemala). The bibliographical data, either primary or secondary, comprise codices (pre-Columbian and Colonial), chronicles (Colonial), Personal diaries (eighteenth and nineteenth centuries), foreign travellers' writings (eighteenth to twentieth centuries), and works from historians and scientists (nineteenth to twentieth centuries). For newspapers, which began to appear in eighteenth century but became more regular with even daily circulation from the beginning of nineteenth century on, the 25 titles reviewed offer primary as well as secondary data,

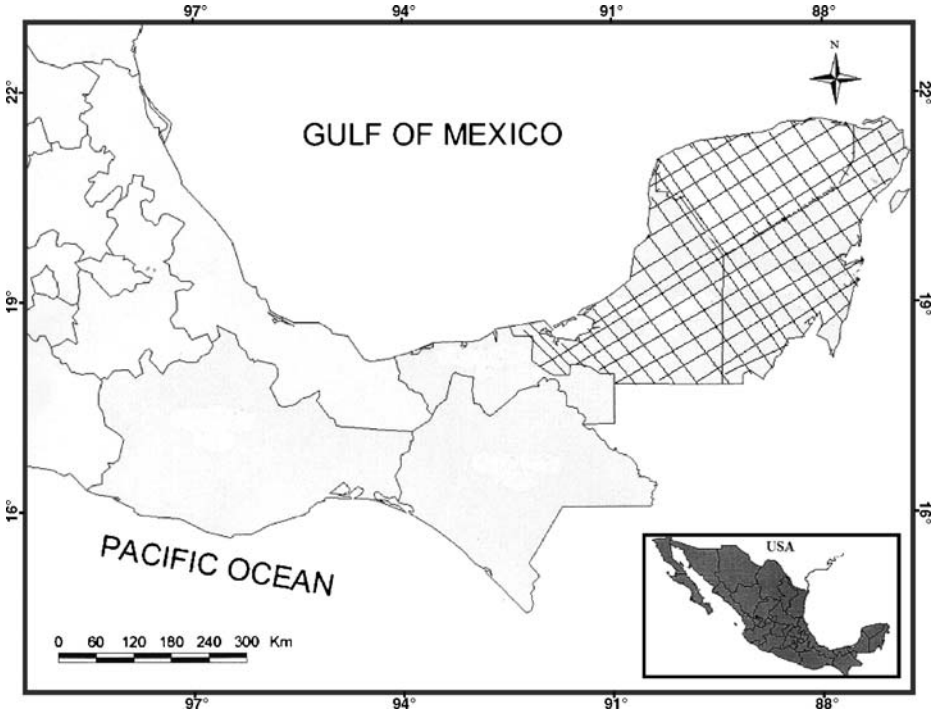

Fig. 1 Area of study

which increases mainly from the second half of nineteenth century onwards. Iconographical sources (known as "exvotos" or retables), which are fewer in quantity, but are compensated by its beauty, refer mainly to events occurred from the middle of nineteenth century onwards.

The Catalogue includes events associated with hydrometeorological phenomena or hazards whose effects were mainly felt in the agricultural sector, and that is why they are called agricultural disasters. Frost, hailstorm, and hurricane records come along with information about water-scarcity or water-surplus that provoked droughts and floods throughout more than five centuries of Mexican history. The term drought (sequía or seca in Spanish) is not very common in former Mexican archival, bibliographical or journalistic documents consulted; it began to be commonly used from the nineteenth century onwards. Before that, primary as well as secondary sources in historical documents refer mainly to scarcity, lack or delay of water and/or rains. Drought records in the Catalogue correspond then to long periods of lack, scarcity or delay of rainfall, to extended periods of time with below normal precipitation.

Droughts as slow impact events make it difficult to identify information in historical sources. Dating the onset and termination of a drought as well as its spatial extent with historical data, mainly qualitative, constitutes a real challenge for the researcher. Droughts may last weeks, months or even years but historical documents, mainly the oldest ones, never indicate it as such. That is why in many cases droughts have to be dated starting with and measuring its effects and impacts. The same happens with other events, which, as droughts, constitute slow impact ones (epidemics), in contrast with sudden impact events (earthquakes or hurricanes) whose beginning and end can be easily identified and recorded.

Table 1 Historical droughts in the Yucatan Peninsula

Starting year	Duration (years)
1535	7
1551	2
1564	1
1571	1
1575	2
1648	1
1650	4
1661	1
1725	3
1765	10
1800	6
1807	1
1809	2
1813	1
1817	1
1822	2
1834	2
1837	1
1842	1
1844	1
1854	1
1881	2
1887	1
1889	2
1896	1

According to the information coming from the Catalogue, it was mostly when the drought was linked to its impact that the phenomenon was actually labelled as such. In agriculture-based economies such as that practiced in Mexico from pre-Columbian times up to the beginning of the twentieth century, the success or failure of the main crops in 1 year was the indicator of the success or failure of the whole economy. "Bad years," currently associated with droughts, happened in periods that historians have identified as "agricultural crises," related mainly to maize crop losses and to the increase of its price as well as that of other basic commodities.

Historical droughts reported in the Catalogue were then severe enough to have seriously affected the population and severe enough to have been recorded in historical documents. It is likely that most of these droughts were anomalous phenomena, i.e. more intense and of longer duration, which had a greater impact on the population than did the quasi year-to-year occurrence of the mid summer drought observed in southern Mexico.

4 Materials and methods

In Fig. 1 we show the area of study that comprises the modern states of Campeche, Yucatan and Quintana Roo, the Yucatan Peninsula or what we have called in this paper the Mexican Maya Lands. The series presents 25 droughts (see Table 1), and was constructed as follows: droughts occurring in adjacent years were counted as a single drought and assigned to the first of the consecutive years, then the number of consecutive years is considered as the

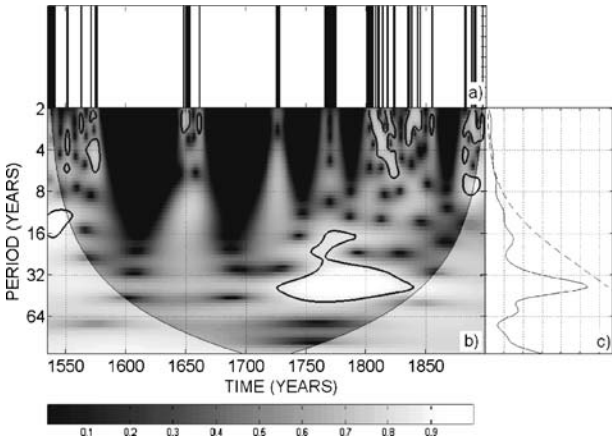

Fig. 2 **a** Historical drought time series; **b** wavelet spectrum, the significance level colour code appears at the bottom of the figure, in particular the 95% significance level is inside the black contours; **c** global wavelet spectrum

duration (or intensity) of the drought. Also droughts reported in the same year in different provinces that are part of the area under study were counted as one drought. In the cases in which historical documents report a drought time span, it is taken as the duration of the drought itself.

We are supposing that within the area under study the climate was homogeneous, therefore a drought reported anywhere in the area occurred in the whole region. We are aware of the fact that climatic inhomogeneities happened and that our supposition in some cases may be inappropriate, introducing an error in the final number of droughts. Nevertheless, the fact that even the area of study underwent many jurisdictional and legal changes, it has been continuously and highly populated along the period of study; this element and the fact that hazards in historical documents (slow or sudden impact ones) are generally reported when they reach a minimum level, indicate that the lack of drought reports is more likely due to the absence of the phenomenon itself, at least as a severe drought, rather than to a reduced number of observers.

The drought historical data were transformed into a series of the pulse width modulation type (1 drought, 0 no drought; Holmes 2003) shown in Fig. 2a as vertical lines. The intensity of the droughts is taken into account by assigning to the pulses a certain width, corresponding to the drought duration in years. Changing the pulse amplitude instead of the width, to assign intensity produced essentially the same results.

It can be useful to investigate the frequencies, if any, that the drought series presents. In order to analyze localized variations of power within a time series at different frequencies we apply the wavelet method. The wavelet method is applicable to a series of pulses as has been shown in other works (Ogurtsov et al. 2002; Hasegawa 2005). In particular we use the Morlet wavelet (Daubechies 1990; Lau and Weng 1995, Grinsted et al. 2004). The Morlet wavelet consists of a complex exponential modulated by a Gaussian, taking advantage of this type of expression, it will be used to calculate the wavelet coherence phase difference.

We estimate the significance level for each wavelet scale using only values inside the cone of influence. The cone of influence is the region of the wavelet spectrum in which edge effects become important and is defined here as the *e*-folding time for the autocorrelation of wavelet power at each wavelet scale. This *e*-folding time is chosen so that the wavelet power for a discontinuity at the edge drops by a factor e^{-2} and ensures that the edge effects are negligible beyond this point. The size of the cone at each scale also gives a measure of the decorrelation time for a single spike in the time series. The cone of

influence in the corresponding wavelet spectrum figures is marked by the curved black lines across the whole figure. By comparing the width of a peak in the wavelet power spectrum with this decorrelation time, one can distinguish between a spike in the data (possibly due to random noise) and a harmonic component at the equivalent Fourier frequency (Torrence and Compo 1998). The global wavelet spectrum is defined by Torrence and Compo (1998) as: $\mathrm{WGS}(s) = \sum_n \left|W_n^X(s)\right|^2$, where $\left|W_n^X(s)\right|^2$ is the wavelet spectrum power with $W_n^X(s)$ as the wavelet transform of the X series. To determine significance levels of the global wavelet power spectrum, one first needs to choose an appropriate background spectrum. For many geophysical phenomena, an appropriate background spectrum is either white noise, with a flat Fourier spectrum, or red noise that presents increasing power with decreasing frequency (Torrence and Compo 1998; Gilman 1963). The dashed curves in the global wavelet spectra indicate the power of the red noise level. The uncertainties of the peaks appearing in the global wavelet spectra are obtained from the peak full width at half maximum.

The cross wavelet analysis was introduced by Hudgins et al. (1993). It is also briefly discussed by Torrence and Compo (1998). It has already been applied to various problems in climatology (Torrence and Webster 1999; Huang et al. 1998; Labat et al. 2000; Pozo-Vazquez et al. 2001).

Following Torrence and Compo (1998), the cross wavelet spectrum of two time series X and Y, with wavelet transforms $W_n^X(s)$ and $W_n^Y(s)$ is:

$$W_n^{XY}(s) = W_n^X(s)\, W_n^{Y^*}(s) \tag{1}$$

where n is the time index, s is the scale and (*) denotes complex conjugation. Further, the cross-wavelet power is defined as: $\left|W_n^{XY}(s)\right|^2$. The phase angle of W^{XY} describes the phase relationship between X and Y in the time–frequency space.

The Fourier squared coherence is used to identify frequency bands within which two time series are covarying. The wavelet squared coherence is a measure of the intensity of the covariance of the two series in time–frequency space, unlike the cross-wavelet power which is a measure of the common power. In the approach of Torrence and Webster (1999), the wavelet square coherence is defined as the absolute value squared of the smoothed cross-wavelet spectrum, normalized by the smoothed wavelet power spectra.

$$R_n^2(s) = \frac{\left|\left\langle W_n^{XY}(s)\right\rangle\right|^2}{\left\langle s^{-1}\left|W_n^X(s)\right|^2\right\rangle \left\langle s^{-1}\left|W_n^Y(s)\right|^2\right\rangle}, \tag{2}$$

where indicates smoothing in both time and scale. The factor s^{-1} is used to convert to an energy density. Also $0 \leq R_n^2 \leq 1$. Moreover, the wavelet coherence phase difference is given by:

$$\varphi_n(s) = \tan^{-1}\left(\frac{\left\{Im\left\langle s^{-1} W_n^{XY}(s)\right\rangle\right\}}{\left\{Re\left\langle s^{-1} W_n^{XY}(s)\right\rangle\right\}}\right) \tag{3}$$

In this work we have further defined the global wavelet coherence spectrum (GWCS) as:

$$\mathrm{GWCS}(s) = \sum_n R_n^2(s) = \sum_n \frac{\left|\left\langle W_n^{XY}(s)\right\rangle\right|^2}{\left\langle s^{-1}\left|W_n^X(s)\right|^2\right\rangle \left\langle s^{-1}\left|W_n^Y(s)\right|^2\right\rangle} \tag{4}$$

Even if the scales were appropriately weighed for the averaging, it is possible for two series to be significant even if its correlation is much less than 5% (Grinsted et al. 2004).

Table 2 Historical droughts and duration

Number of events	Duration (years)
14	1
6	2
1 (1725–1727)	3
1 (1650–1653)	4
1 (1800–1805)	6
1 (1535–1541)	7
1 (1765–1774)	10

Only coherences of 0.5 or larger appear in the corresponding figures, however, we shall discuss mainly those frequencies that are significant at the 95% confidence level.

The statistical significance level of the wavelet coherence is estimated using Monte Carlo methods with red noise to determine the 5% statistical significance level of the coherence (Torrence and Webster 1999). The Monte Carlo estimation of the significance level requires of the order of 1,000 surrogate data set pairs (Grinsted et al. 2004). Empirical testing indicates that the colour of the noise (determined by the first order autoregressive coefficients of the two original time series) has no influence on the magnitude of the coherence corresponding to the 5% significance level, whereas the specifics of the smoothing operator have a large influence (Torrence and Webster 1999).

The arrows in the coherence spectra show the phase between the phenomena, arrows at 0° (horizontal right) indicate that both phenomena are in phase and arrows at 180° (horizontal left) indicate that they are in anti-phase, it is very important to point out that these two cases imply a linear relation between the considered phenomena; arrows at 90° and 270° (vertical up and down, respectively) indicate an out of phase situation which means that the two phenomena have a non-linear relation.

We would like to point out that the wavelet coherence is especially useful in highlighting the time and frequency intervals where two phenomena have a strong interaction.

5 Results

According to Table 2, throughout the Mexican Maya lands from the sixteenth to nineteenth centuries 14 droughts lasted only 1 year and six more lasted 2 years; the remaining lasted 3, 4, 6, 7 and 10 years. In particular the 7-year drought, the first in our area of study between 1535 and 1541, is linked to locust plague and with hunger and death: “las lluvias faltaron por completo, o fueron excesivamente escasas, y de aquí dimanó una gran sequía que hizo perder las cosechas de cereales, apareció por distintos lugares la espantosa plaga de langostas, la cual, acabó instantáneamente con las pocas sementeras formadas en los lugares que no estuvieron completamente privados de lluvia.”[1] (García-Acosta et al. 2003:96).

According to Fig. 2a, five conspicuous time lapses with no droughts occurred between 1577–1647, 1662–1724, 1728–1764, 1774–1799 and 1855–1880. On the other hand the epochs with most frequent droughts were between 1800 and 1850. Figures 2b–c show four

[1] “The rains were altogether absent, or were highly deficient, and from that emerged a great drought, which led to the loss of the grain harvest, accompanied by plagues of locusts, which in turn decimated those few fields that had received some meagre rains.”

Table 3 Summary of coherence spectra results for the Yucatan Peninsula

Frequency (years)	SC	AMO	SOI	TSI	^{10}Be
6			1650–1670 (anti) 1720–1740 (in) 1820 (out) 1850 (in) 1870–1900 (out)		
7		1650–1675 (anti) 1760–1780 (out) 1870–1900 (anti)			
11				1640–1670 (in) 1700–1730 (out) 1820–1840 (anti)	
12	1630–1680 (out) 1720–1740 (anti) 1830–1850 (out)				
13					1640–1680 (in) 1720–1740 (in) 1830–1840 (in)
14		1715–1740 (in) 1780–1800 (out)	1700–1740(out) 1800–1840 (in)		
20				1640–1670 (anti) 1770–1790 (in) 1830–1850 (anti)	
24					
32				**1670–1700 (out)** **1750–1830** **(anti–out)**	1630–1680 (anti–out) 1870–1900 (in)
40	**1720–1850 (anti)**	**1750–1850 (anti)**			
48			**All period (in)**		
60				**1800–1850 (anti–out)**	
64	**All period (in)**				**All period (in)**

The bold letters correspond to the frequencies with the maximum power.

SC Sediment cores; *AMO* Atlantic Multidecadal Oscillation; *SOI* Southern Oscillation Index *TSI* Total Solar Irradiance; ^{10}*Be* the Berilium 10 isotope. *(in)* In-phase; *(out)* out of phase; *(anti)* anti-phase.

prominent periodicities of the drought series around 11±2, 20±4, 40±4 and 56±4; the most important one being that of ~40 years. The 40 years periodicity is close but below the red noise level in the global wavelet spectrum (Fig. 2c), however, in the spectral wavelet plot (Fig. 2b) it is at the 95% confidence level between 1730 and 1840, and no other frequency in this plot reaches such level.

Applying a simple correlation to the series of droughts and the various indices we are using, we obtained very low correlation coefficients, the reason is that for some time periods they correlate and for some others they do not correlate; therefore we take advantage of the characteristics of the wavelet squared coherence, described in Section 4, to find the interactions between two phenomena. Table 3 shows a summary of results.

Figure 3a compare the historical droughts with droughts inferred from multiple sediment cores in a Yucatan lake (Hodell et al. 2004). From the upper panel of Fig. 3a we notice that the droughts tend to appear around increases of gypsum concentrations, indicating increased aridity in the region. Moreover, the gypsum concentration is higher for the time lapse of 1780–1900 than for previous years, this comprises also the epoch of higher drought

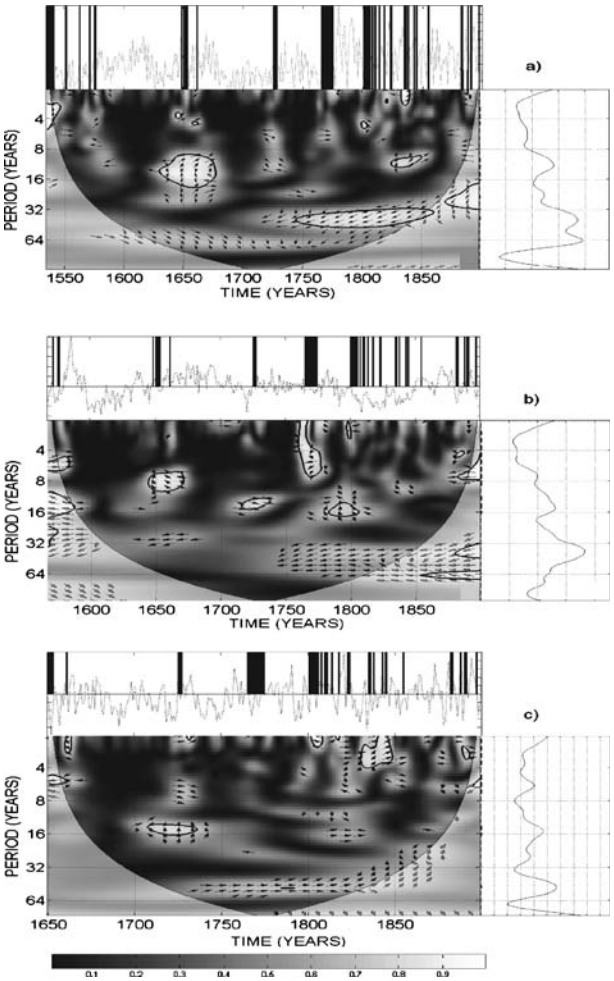

Fig. 3 Coherence spectrum between historical droughts in the Yucatan peninsula and **a** Sediment lake cores; **b** Atlantic Multidecadal Oscillation; **c** Southern Oscillation Index. The *direction of the arrows* in the coherence spectrum indicates the phase between the two phenomena involved: horizontal right is 0° and correspond to an in-phase situation, horizontal left is 180°, and correspond to an anti-phase situation, both situations imply a linear relation between the phenomena; *vertical up (90°) and vertical down (270°) arrows* correspond to an out-of phase situation, i.e., a non-linear relation. The *arrows* are plotted every 12 years. The *upper panel* of each figure shows the time series of the data involved. The significance level colour code appears at the bottom of the figure, in particular the 95% significance level is inside the black contours

occurrence. The lower panel of Fig. 3a shows the coherence between droughts and sediment cores. The strongest coherence is evident for frequencies of ~40 and 64 years. However ~40 years increase of gypsum tend to correspond to decreases of droughts along 1750–1850, while at ~64 years they tend to follow each other.

Large scale climate modes are for instance the changing conditions of the North Atlantic sea surface temperature, that present multidecadal variability over the last 150 years (Schlesinger and Ramankutty 1994). The leading mode of low-frequency changes of the North Atlantic sea surface temperature is known as the Atlantic Multidecadal Oscillation (AMO; Kerr 2000). The AMO shows frequencies in the range of 65 to 80 years. The AMO has been linked to precipitation anomalies over North America, appears to modulate the El Niño–Southern Oscillation (ENSO) teleconnections over large parts of the Northern Hemisphere (McCabe et al. 2004), also it seems to play a role in Atlantic hurricane formation, African drought frequency and European winter temperatures (Folland et al. 1986; Goldenberg et al. 2001). To our knowledge there are no studies concerning specifically the AMO and precipitation (or drought) in the Yucatan Peninsula. A related study was performed by Jáuregui (1979), who showed that for the period 1915–1972 the decrease in

the intensity of the trade winds coincided with lower than normal precipitation in central of Mexico. The trade winds are closely related to the North Atlantic Oscillation (NOA), which is one of the most prominent patterns of atmospheric circulation variability; moreover, the AMO is related to the NAO (Gray et al. 2004). Although the area of study is far from the so-called centres of influence in the North Atlantic, there seems to be a certain influence of the NOA on precipitation variability in the Yucatan peninsula as derived from the Northern Hemisphere winter maps presented by Jones et al. (2003). As instrumental records exist since 1856, in order to assess the effect of the AMO on historical droughts in the Yucatan Peninsula we use a recent tree-ring AMO reconstruction since 1567 (Gray et al. 2004).

Figure 3b compares the historical droughts with the AMO. From this panel we notice a tendency for droughts and the cold phase of the AMO to nearly coincide throughout most of the study period, particularly from about 1750 to 1850 that comprises the time span with the highest drought rate occurrence. Coherence is particularly strong around the 40-year time scale with both SOI and AMO (lower panels), and clearly indicates that droughts occur during the cold phase of the AMO (they are anti-correlated).

The most important mode of climate variability in the equatorial Pacific is El Niño–Southern Oscillation: the warm and cold phases of the sea surface temperature are known as El Niño and La Niña, respectively, and the changes in atmospheric pressure are the Southern Oscillation Index (SOI). El Niño–precipitation relationships have been examined for tropical and extra tropical regions (e.g., Ropelewski and Halpert 1986, 1989). Given the large latitudinal extent of Mexico in the tropics/subtropics, Cavazos and Hastenrath (1990) have explored the role of the El Niño for various rainfall regimes in Mexico; large regions of the north and centre of Mexico appear to be correlated to El Niño in this study. In an attempt to detect a link between the historical El Niño series by Quinn and Neal (1992) and a historical drought series (1535–1987) for the whole country published by Florescano (1980), Jáuregui (1995) found that the highest frequency of droughts reported in some regions of Mexico for 1822–1987 occurred in El Niño years at a 0.5% significance level under a Chi-square test. Generally speaking in Mexico El Niño produces more precipitation in the north and centre of the country and less precipitation towards the south (Magaña et al. 2003).

Mendoza et al. (2006) performed a study of historical droughts in southeastern Mexico, using the Garcia-Acosta et al. (2003) catalogue, and El Niño events, using the Quinn and Neal (1992) and the Ortlieb (2000) compilations. The period of study was 1502–1899. El Niño events were associated to droughts grouped by El Niño intensities. In order to evaluate the statistical confidence of the results they applied the Chi-square test (χ^2) to the distribution of droughts 3 years before and 3 years after the occurrence of El Niño. They found that at most 38% of droughts are confidently related to El Niño events. Since the precipitation regime in this region is mostly determined by tropical disturbances, e.g. easterly waves, tropical storms and hurricanes, during the rainy season (Jáuregui 1995) it is possible that the impact of these weather systems on the rainfall regime of southeastern Mexico may be generally less influenced by the El Niño phenomenon than in other parts of the country, were historically droughts have been linked to El Niño (Jáuregui 1995). Furthermore, in the study of the Palmer Drought Severity Index (PDSI) and El Niño events along 1921–1987 carried out by Herrera (2005), the author found that in the Yucatan Peninsula the association between the two series is very low; nevertheless, the most prolonged and severe droughts, those occurring ~1942–1946 and ~1949–1952, coincided with strong El Niño events.

Instrumental records of the phenomenon, either atmospheric or oceanic, extend back to 1867. To relate historical droughts and the SOI, we use a tropical multiproxy SOI reconstruction since 1650 (Jones and Mann, 2004). In Fig. 3c (lower panel) for droughts

and the SOI we notice that the strongest coincidence is for the frequencies of ~48 years, also that during the positive phase of the SOI there are more droughts, this means that droughts are not highly associated to El Niño events, because this phenomenon is related to the negative SOI phase.

The relation of droughts in the Yucatan peninsula with solar activity is analyzed in Fig. 4 (see also Table 3 for a summary of results). Figure 4a shows that the strongest coherence between droughts and Total Solar Irradiance (TSI; Lean 2000) is found ~32 and 60 years. For these frequencies more droughts tend to occur during times of lower irradiance. Figure 4b shows the coherence between droughts and the isotope Be^{10} (Beer 2000). Cosmic rays are highly energetic particles coming from outside the solar system. Upon entering the solar system they are modulated by solar activity in such a way that during solar maximum activity times the flux entering the Earth atmosphere diminished and during maximum epochs it increases. When cosmic rays enter the atmosphere they interact with its constituents producing isotopes such as Be^{10}. The strongest coherence with Be^{10} is found at ~64 years, indicating that there are more droughts at times of higher cosmic ray flux. Higher cosmic ray flux epochs are also times of diminished TSI, and this behavior is consistent with the results found for droughts and TSI in Fig. 4a.

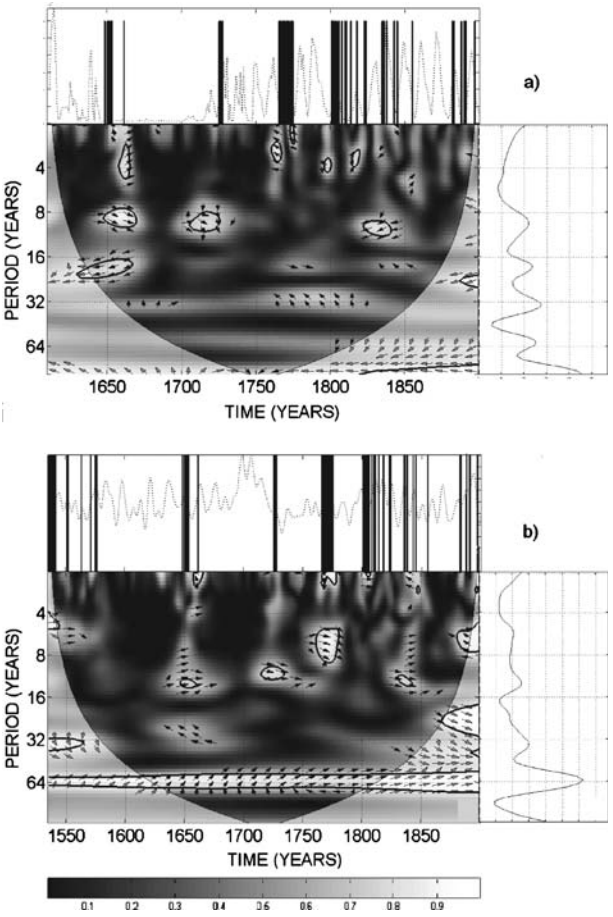

Fig. 4 Coherence spectrum for the historical droughts and **a** total solar irradiance; **b** ^{10}Be. The key for the *arrows* and colour code are the same as in Fig. 3. The *upper panel* of each figure shows both time series of data

6 Modern drought in the Yucatan Peninsula

Figure 5a shows the time series of the PDSI for the Yucatan Peninsula. We use the PDSI, calculated by Herrera (2005) for the Yucatan Peninsula during the period 1921–1987. Severe droughts are defined as those with PDSI values ≤−4. Severe droughts appeared eight times in the period 1927–1988. The most prominent negative phases occurred between ~1942–1946 and 1949–1952, with durations of roughly 4 and 3 years, respectively. Other times presenting strong negative phases are ~1923–1924, 1928–1929, 1935–1936, 1962–1963,1971–1972 and 1986–1987.

In Figs. 5b and c we present the spectral analysis of the PDSI. Two prominent periodicities clearly appear: ~5.5±0.5 and the strongest of 10±2 years. They could be associated either to ENSO events or to solar activity.

Figure 6a shows the coherence between the PDSI and the AMO, three frequencies are most evident: ~3, 10 and the most evident at ~23 years. The first one appears prominently near 1925, (in anti-correlation) and along 1941–1948 (an out of phase situation), the 10 and 23 years frequency are present along the entire period, indicating that droughts occurred during both the cold and warm phases of the AMO. This suggests there has been no consistent association between PDSI and AMO during the instrumental record. Figure 6b indicates that the SOI and the PDSI have coincidences at ~5, 10 and the most prominent at ~22 years, the first frequency is prominent around 1954–1960 and 1970–1977, the other two appear during the full period. With regards to the phase, a non-linear relation between droughts and SOI is present. The PDSI is in phase with both AMO and SOI mainly at ~23 years, which is the most prominent frequency in both coherence spectra. However, we would like to point out that due to the length of the series the 23 years frequency is mostly outside the cone of influence. The other period of relatively high coherence is ~10 years; at this frequency (see Fig. 6) the AMO has a more linear relation with droughts than the SOI.

Figure 7a shows the coherence between the PDSI and sunspots (Royal Observatory of Belgium (http://sidc.oma.be), two frequencies are most evident: ~8, 20 years. They appear along all the period. We notice that droughts and sunspots (that follow quite closely the TSI) behave in a similar way as historical droughts and the TSI do at these frequencies (see Fig. 5a), i.e. they tend to correlate. Figure 7b indicates that the PDSI and cosmic rays have coincidences at ~1 and 8 years, presenting an out of phase situation.

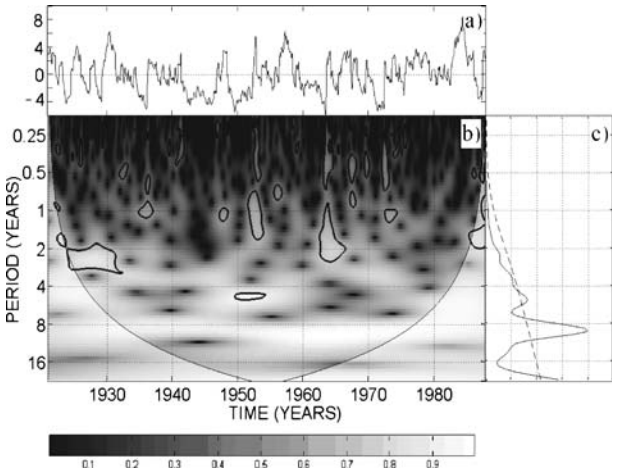

Fig. 5 Figure 2**a** Palmer Drought Severity Index time series; **b** wavelet spectrum, the colour code is the same as in Fig. 2b; **c** global wavelet spectrum

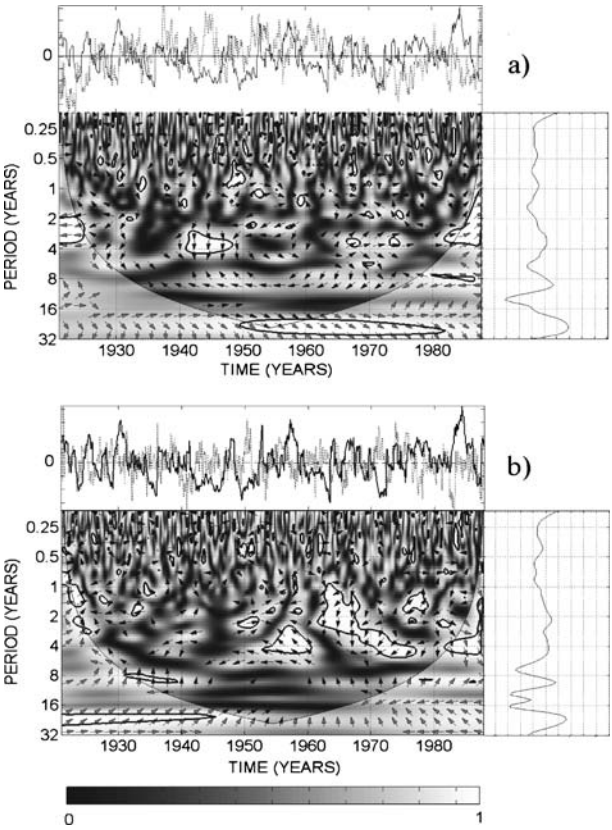

Fig. 6 Coherence spectrum between the Palmer Drought Severity Index (PDSI) series and, **a** Atlantic Multidecadal Oscillation (AMO), **b** Southern Oscillation Index. The key for the *arrows* and the colour code are the same as in Fig. 3. The *upper panel* of each figure shows both time series of data with the PDSI depicted as the solid curve in both cases

7 Effects and impacts on Maya society

The above mentioned historical drought series indicates that over a period of more than three and a half centuries, a total of 25 severe droughts were recorded, and these events lasted from 1 to 10 years. As has been stated before, they were severe enough as to have been recorded in historical documents.

In agriculture-based societies a severe drought and a high losses of basic commodities associated with often led to generalized crises. Drought effects and impacts accumulated throughout different time intervals. These events are sometimes described as "creeping environmental phenomena," but the magnitude of effects and impacts resulting from them were commensurate with the drought frequency and duration. The more recurrent effects and impacts in historically recorded droughts in Mexican Maya Lands region, besides water scarcity in general, were linked to crop failure that could reach 100%, followed by shortage and higher prices of basic commodities, mainly corn. Temporary or permanent migration came after.

In extreme cases, hunger and the spread of diseases mainly among the indigenous population, the Maya inhabitants of the region, led to famine and death. Nevertheless it has to be stated that death was more associated with the spread of diseases and epidemics, than with the food shortage itself. Vulnerability within certain social sectors associated with hunger, made them the easiest victims to disease, epidemics and death.

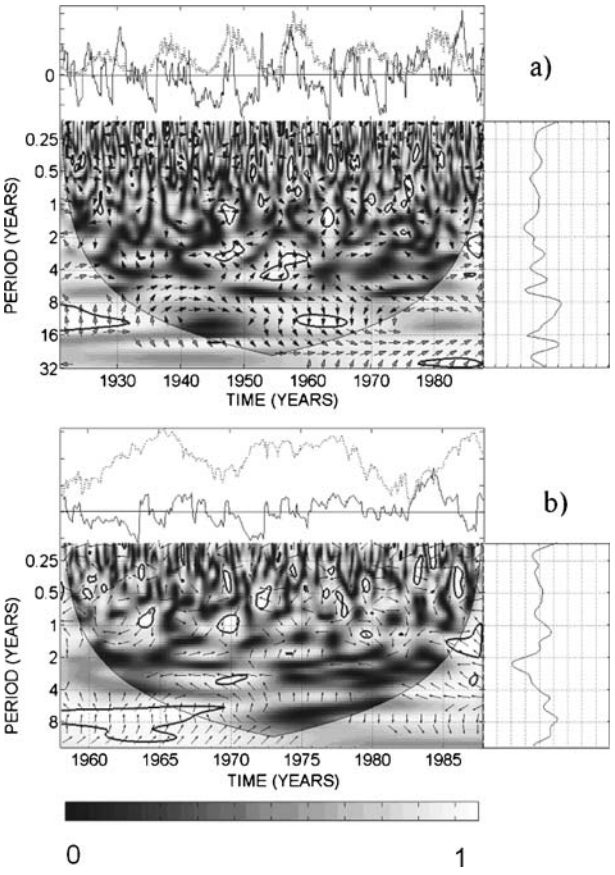

Fig. 7 Coherence spectrum for the Drought Palmer Index and **a** sunspot number monthly data from the Royal Observatory of Belgium for the period 1921–2006 (http://www.sidc.be); **b** cosmic ray monthly data from the Moscow Neutron Monitor for the period 1958–2006 (http://helios.izmiran.troitsk.ru/cosray/main.htm). The key for the *arrows* and the colour code are the same as in Fig. 3. The *upper panel* of each figure shows both time series of data

If it is true that there are different ways through which societies have adapted to their environment, in Maya Lands the diachronic approach in face of natural hazards have taught us several lessons. As in other Mexican regions, certain factors have led to increase the effects and impacts of droughts. Environmental degradation, destruction of basins, changes in agricultural practices, pollution of aquifers have been, among others, part of the social construction of risks that coupled with an growing vulnerability has led to increasing the effects and impacts of natural hazards mainly among certain social sectors.

8 Discussion and conclusions

The historical drought series indicates that in a lapse time of 365 years 25 severe droughts occurred, an average of 0.07 droughts per year. In particular, between 1535 and 1800 there were 10 severe droughts, an average of 0.04 droughts per year, and from 1800 to 1900 there were 15 severe droughts, 0.15 droughts per year. The modern series shows that along 66 years eight severe droughts occurred, an average of 0.12 droughts per year. As the modern series finishes in 1988, we can only say that in the first 66 years of the twentieth century the severe drought occurrence rate is lower compared with the nineteenth century.

These droughts had differential effects and impacts among the Maya Lands inhabitants, which, in the most critical ones and as a result of the association of crop failure, hunger, spread of diseases and epidemics, leading to high mortality among the more vulnerable Mayas.

Most of modern and historical droughts lasted 1 year, however, no modern drought lasted more than 4 years, while we have historical droughts lasting 6, 7 and 10 years. Also, modern and historical droughts present a quasi-decadal frequency.

Comparison of historical droughts with proxy climate records showed a tendency for them to occur around higher concentrations of gypsum, obtained from lake sediment cores. Based on the technique of wavelet spectrum analysis, historical droughts had weaker coherence with the SOI than with the AMO, although statistical significance of these associations is sustained during most of the time interval, 1730–1850. In a previous study carried out on historical droughts and El Niño in southern Mexico, Mendoza et al. (2006) pointed out that these phenomena exhibited a moderate association, Modern droughts seem to be equally associated with both AMO and SOI, however the coherence seems to be more sustained with the AMO. The strongest coincidences between historical droughts and AMO and SOI occurred around the same periodicities (40–48 years), while modern droughts coincide with AMO and SOI mainly at ~10 years.

Concerning the solar activity proxies and historical droughts, clearly the coherence with Be^{10} (cosmic rays) is higher than with TSI, and is very persistently present along time. We notice that the strongest coherence between droughts and TSI and Be^{10} occurs for both solar activity proxies at periods ~60–64 years. When studying modern droughts and solar activity, the coherence is strongest ~8 years, but it seems to be equally important for both sunspots and cosmic rays, although for the sunspots seems to be more sustained in time.

Comparing natural terrestrial and solar phenomena, we realize that the strongest modulation of historical drought occurrence is at the low frequency band of ~60–64 years and is between droughts and the solar proxy Be^{10}, it is also notably sustained in time. For modern droughts we notice that the coherence with all four phenomena seems to be similar and it is found at ~8–10 years.

We can conclude that Atlantic sea surface temperatures variations as depicted by the AMO and the indicators of solar activity have influenced drought in the Mayan region of southern Mexico. The long-term influence of the SOI appears to be less consistent than that of the AMO.

References

Beer J (2000) Long-term indirect indices of solar variability. Space Sci Rev 94:53–66

Bracamonte P (1994) La memoria enclaustrada. Historia indígena de Yucatán, 1750–1915, Historia de los pueblos indígenas de México, CIESAS and INI, México, 253 pp

Cavazos T, Hastenrath S (1990) Convection and rainfall over Mexico and their modulation by the Southern Oscillation. Int J Climatol 10:377–386

Colle B, Moss C (1995) The structure and evolution of cold surges east of the Rocky Mountains. Mon Weather Rev 123:2577–2610

Daubechies I (1990) The wavelet transforms time–frequency localization and signal analysis. IEEE Trans Inf Theory 36:901–1004

Di Mego J, Basart L, Endersen W (1976) An examination of the frequency and mean conditions surrounding frontal incursions into the Gulf of Mexico and Caribbean Sea. Mon Weather Rev 104:709–718

Escobar A (2004) Desastres agrícolas en México. Catálogo histórico. Tomo II: Siglo XIX (1822–1900). Fondo de Cultura Económica and CIESAS, México, 280 pp

Farriss NM (1992) La sociedad maya bajo el dominio colonial. Alianza Editorial, Madrid, 653 pp

Florescano E (1980) Análisis históricos de las sequías en México. SARH Committee Plan Hidráulico Nacional, México
Folland CK, Palmer TN, Parker DE (1986) Sahel rainfall and worldwide sea temperatures. Nature 320:602–606
García-Acosta V, Pérez-Zevallos JM, Molina del Villar A (2003) Desastres agrícolas en México. Catálogo histórico. Tomo I: Épocas prehispánica y colonial (958–1822). Fondo de Cultura Económica and CIESAS, México, 506 pp
Gilman DL, Fuglister FH, Mitchell JM (1963) On the power spectrum of "red noise." J Atmos Sci 20:182–-184
Goldenberg SB, Landsea CW, Mestas-Nuñez AM, Gray WM (2001) The recent increase in Atlantic hurricane activity: causes and implications. Science 293:474–479
Gray ST, Graumlich LJ, Betancourt JL, Pederson GT (2004) A tree-ring based reconstruction of the Atlantic Multidecadal Oscillation since 1567 A.D. Geophys Res Lett 31:L12205–L12208
Grinsted A, Moore J, Jevrejera S (2004) Application of the cross wavelet transform and wavelet coherence to geophysical time series. Nonlinear Process Geophys 11:561–566
Hasegawa H (2005) A wavelet analysis of transient spike trains of Hodgkin–Huxley neurons. http://arxiv.org/ps/cond-mat/0109444
Herrera G (2005) Caracterización Geográfica de la Sequía en México. Ph.D. thesis, Universidad Nacional Autónoma de México, Facultad de Filosofía y Letras, Colegio de Geografía
Hodell DA, Brenner M, Curtis JH (2004) Terminal classic drought in the northern Maya lowlands inferred from multiple sediment cores in lake Chichancanab (Mexico). Quat Sci Rev. doi: 10.1016/j.quascirev.2004.10.013
Holmes DG (2003) Pulse width modulation for power converters: principles and practice. Thomas A. Lipo, 724 pp
Huang J, Higuchi K, Shabbar A (1998) The relationship between the North Atlantic Oscillations and El Niño-Southern Oscillation. Geophys Res Lett 25:2707–2710
Hudgins L, Friebe C, Mayer M (1993) Wavelet transforms and atmospheric turbulence. Phys Rev Lett 71:3279–3282
Jáuregui E (1979) Some aspects of pluviometric fluctuations in Mexico during the last 100 years (in Spanish). Bol Inst Geogr (UNAM) 9:39–64
Jáuregui E (1995) Rainfall fluctuations and tropical storm activity in Mexico. Erdkunde 49:39–48
Jáuregui E (1997) Climate changes in Mexico during the historical and instrumental periods. Quat Int 7:43–44
Jones PD, Mann ME (2004) Climate over past millennia. Rev Geophys 42(2):RG2002, doi: 10.1029/2003RG000143
Jones PD, Osborn TJ, Briffa KR (2003) Pressure-based measures of the North Atlantic Oscillation (NAO): a comparison and an assessment of changes in the strength of the NAO and in its influence on surface climate parameters. In: Hurrell JW, Kushnir Y, Ottersen G, Visbeck M (eds) The North Atlantic Oscillation, climate significance and environmental impact. Geophys Monogr 134:51–62
Kerr RA (2000) A North Atlantic climate pacemaker for centuries. Science 288:1984–1986
Klaus D (1973) Cold polar outbreaks in the tropics forming on the leeward of the Rocky Mountains. Geofis Int 13:99–143 (in Spanish)
Labat D, Ababou R, Mangin A (2000) Rainfall-runoff relations for karstic springs. Part II: continuous wavelet and discrete orthogonal multiresolution. J Hydrol 238:149–178
Lean J (2000) Evolution of the Sun's spectral irradiance since the Maunder minimum. Geophys Res Lett 27:2425–2428
Lau K-M, Weng H-Y (1995) Climate signal detection using wavelet transform: how to make a time series sing. Bull Am Meteorol Soc 76:2391–2402
Magaña V, Amador J, Medina S (1999) The midsummer droughts over Mexico and Central America. J Climate 12:1577–1588
Magaña V, Vázquez J, Pérez J, Pérez JB (2003) Impact of el Niño on precipitation in Mexico. Geofis Int 42:313–330
McCabe G, Palecki M, Betancourt JL (2004) Pacific and Atlantic Ocean influences on multi-decadal drought frequency in the United States. Proc Natl Acad Sci U S A 101:4136–4141
Mendoza B, Jáuregui E, Díaz-Sandoval R, García-Acosta V, Velasco V, Cordero G (2005) Historical droughts in central Mexico and their relation with El Niño. J Appl Meteorol 44:709–716
Mendoza B, Velasco V, Jáuregui E (2006) A study of historical droughts in southeastern Mexico. J Climate 19:2916–2934
Mosiño P, García E (1966) The midsummer droughts in Mexico. In: Proc. Regional Latinamerican Conference, Int. Geophys. Union, Latin American Chapter 3, pp 500–516
Ogurtsov MG, Nagovitsyn YuA, Kocharov GE, Jungner H (2002) Long-period cycles of the sun's activity recorded in direct solar data and proxies. Sol Phys 211:371–394

Ortlieb L (2000) The documented historical record of El Niño events in Peru: An update of the Quinn record (sixteenth through nineteenth centuries). In: Diaz HF, Markgraf V (eds) El Niño and the Southern Oscillation Multiscale Variability and Global and Regional Impact. Cambridge University Press, pp 207–295

Pozo-Vazquez D, Esteban-Parra M, Rodrigo F, Castro-Diez Y (2001) A study of NAO variability and its possible non-linear influences on European surface temperature. Clim Dyn 17:701–715

Quinn WH, Neal VT (1992) The historical record of El Niño events. In: Bradley RS, Jones PD (eds) Climate since A.D. 1500. Routledge, London, pp 623–648

Ropelewski C, Halpert M (1986) North American precipitation and temperature patterns associated with El Niño/Southern Oscillation (ENSO). Mon Weather Rev 114:2353–2362

Ropelewski C, Halpert M (1989) Precipitation patterns associated with the high phase of the Southern Oscillation. J Climate 2:268–284

Schlesinger ME, Ramankutty N (1994) An oscillation in the global climate system of periods 65–70 years. Nature 367:723–726

Schultz D, Bracken E, Bosart L, Hakim G, Bedrick M, Dickinson M, Tyle K (1997) The 1993 superstorm cold surge frontal structure and tropical impact. Mon Weather Rev 125:5–39

Torrence C, Compo G (1998) A practical guide to wavelet analysis. Bull Am Meteorol Soc 79:61–78

Torrence C, Webster P (1999) Interdecadal changes in the ENSO–monsoon system. J Clim 12:2679–2690